Piezoelastic Behavior of Adaptive Composite Plate with Integrated Sensors and Actuators

Hanen Mallek[2](✉), Hana Mellouli[2], Hanen Jrad[2], Mondher Wali[1,2], and Fakhreddine Dammak[2]

[1] Department of Mechanical Engineering, College of Engineering, King Khalid University, Abha, Saudi Arabia
mondherwali@yahoo.fr

[2] Laboratory of Electromechanical Systems (LASEM), National Engineering School of Sfax, University of Sfax, Route de Soukra km 4, 3038 Sfax, Tunisia
{hanen.mallek, hana.mellouli, Fakhreddine.dammak}@enis.tn, hanen.j@gmail.com

Abstract. This paper is concerned with a piezoelectric shell element to analyze smart structures. The finite element formulation is based on discrete double directors shell elements. The implementation is applicable to the analysis of laminated shells with integrated piezoelectric layers. The third-order shear deformation theory is used in the present method to remove the shear correction factor and improve the accuracy of transverse shear stresses. The element has four nodes with eight nodal degrees of freedoms: three displacements, four rotations and one electric potential, which is assumed to be a linear function through the thickness of each active sub-layer. The piezoelastic behavior of smart composite plate is examined. The obtained results are compared to existing solutions available in literature. An excellent agreement among the results confirms the high accuracy of the current piezoelastic model.

Keywords: Piezoelastic behavior · Double directors' shell element · Sensors/actuators · Piezoelectric material

1 Introduction

Smart structures are considered as new design philosophy and engineering approach that integrates the actions of distributed actuators and sensors into the structural system (Marinković et al. 2006; Rama et al. 2018; Jrad et al. 2018; Mallek et al. 2019a, b). In recent years, the study of these structures has attracted many researchers because of their potential for use in advanced aerospace as well as hydro space, nuclear and automotive structural applications due to their excellent electromechanical properties, easy fabrication, design flexibility, and efficiency to convert electrical energy into mechanical energy (Foda et al. 2010; Chesne and Pezerat 2011; Zhang et al. 2011; Rama 2017; Gabbert 2002). In fact, their intrinsic electromechanical coupling effect

A. Benamara et al. (Eds.): CoTuMe 2018, LNME, pp. 77–84, 2019.
https://doi.org/10.1007/978-3-030-19781-0_10

produces mechanical deformations under the application of electrical loads (i.e. the direct effect) and electrical fields under the application of mechanical loads (i.e. the converse effect).

Modeling a linear analysis of intelligent structures using First order Shear Deformation Theory (FSDT) is widespread in the literature. Neto et al. (2012) proposed a 3-node finite shell element to predict piezoelastic static and dynamic response of smart laminated structures. Recently, another 3-node shell element is developed by Marinković and Rama (2017) in order to predict the static and dynamic response of piezoelectric laminated composite shells. The enhancements in the form of strains smoothing technique and discrete shear gaps were applied in this element formulation. Lammering and Yang (2009) also presented a 4-node degenerate shell elements based on the FSDT. This element is implemented according to the two-field formulation with linearly distributed electric potential.

Nevertheless, FSDT theory does not allow a good analysis through the thickness because it considers constant transverse shear strains across the thickness. This theory requires the introduction of transverse shear correction factors which can be restrictive and may cause inaccuracies. This limitation can be overcome using High order Shear Deformation Theory HSDT (Valvano and Carrera 2017) or modified FSDT theory (Mellouli et al. 2019a; Trabelsi et al. 2018). Higher-order theories take into account the variations of in-plane displacements, transverse shear deformation and transverse normal strain depending in thick structures, through the thickness, without the need for any shear correction coefficients. Investigations using the HSDT model have proved their excellent performance in several studies including the modeling of thick piezo-laminated structures and sandwich structures (Sudhakar and Kamal 2003; Correia et al. 2002; Wu et al. 2002).

Some investigations concerning the linear and nonlinear analysis of shell structures in areas like static, free vibration, and forced vibration of FGM and FG-CNT structures, using discrete double directors shell elements, have been reported in the literature (Mallek et al. 2018; Zghal et al. 2017; Frikha et al. 2016; Wali et al. 2015; Mellouli et al. 2019b). Inspired from these investigations, the piezoelastic response of laminated structures with integrated smart layers is elaborated in this paper, using 3D- piezoelectric shell model based on a discrete double directors shell elements.

2 Theoretical Formulations

The piezoelectric double directors finite shell element is developed in this section, based on the kinematics of high order shear deformation theory. The initial C_0 and the deformed C_t configurations of the shell is assumed to be smooth, continuous and differentiable. Variables associated to C_0 (respectively C_t) are denoted by upper-case letters (respectively lower-case letters). Vectors and tensors are expressed using bold letters.

2.1 Kinematic Assumptions

Considering the hypothesis of a double director shell model, the position vector of any material point (q) in the deformed configuration C_t defined in terms of curvilinear coordinates $\boldsymbol{\xi} = (\xi, \eta, \varsigma = z)$ is given as:

$$\boldsymbol{x}_q(\xi,\eta,z) = \boldsymbol{x}_p(\xi,\eta) + f_1(z)\boldsymbol{d}_1(\xi,\eta) + f_2(z)\boldsymbol{d}_2(\xi,\eta), z \in [-h/2\,,\, h/2] \tag{1}$$

where p represents the material point located on the midsurface surface of the shell, $\boldsymbol{d}_1$ and $\boldsymbol{d}_2$ are the unit shell director vectors and h is the thickness.

The general functions $f_1(z)$ and $f_2(z)$ which reflects a double director's theory can be expressed in function of the thickness variable as follows:

$$f_1(z) = z - 4z^3/3h^2 \;\;,\;\; f_2(z) = 4z^3/3h^2 \tag{2}$$

The vectors of membrane, bending and shear strains are given by:

$$\boldsymbol{e} = \begin{Bmatrix} e_{11} \\ e_{22} \\ 2e_{12} \end{Bmatrix}, \boldsymbol{\chi}^k = \begin{Bmatrix} \chi_{11}^k \\ \chi_{22}^k \\ 2\,\chi_{12}^k \end{Bmatrix} \;, \boldsymbol{\gamma}^k = \begin{Bmatrix} \gamma_1^k \\ \gamma_2^k \end{Bmatrix} \;, k = 1,2 \tag{3}$$

These virtual components are computed in the initial configuration C_0 as:

$$\begin{cases} \delta e_{\alpha\beta} = 1/2\left(\boldsymbol{A}_\alpha.\delta\boldsymbol{x}_{,\beta} + \boldsymbol{A}_\beta.\delta\boldsymbol{x}_{,\alpha}\right) \\ \delta\gamma^k = \boldsymbol{A}_\alpha.\delta\boldsymbol{d}_k + \delta\boldsymbol{x}_{,\alpha}.\boldsymbol{d}_k; \quad \alpha,\beta = 1,2; \quad k = 1,2 \\ \delta\chi_{\alpha\beta}^k = 1/2\left(\boldsymbol{A}_\alpha.\delta\boldsymbol{d}_{k,\beta} + \boldsymbol{A}_\beta.\delta\boldsymbol{d}_{k,\alpha} + \delta\boldsymbol{x}_{,\alpha}.\boldsymbol{d}_{k,\beta} + \delta\boldsymbol{x}_{,\beta}.\boldsymbol{d}_{k,\alpha}\right) \end{cases} \tag{4}$$

The electrical field $\boldsymbol{E}$ is evaluated based on the gradient of the electric potential φ. Its expression is given by:

$$\boldsymbol{E} = -\varphi_{,\alpha}, \; \alpha = 1..3 \tag{5}$$

2.2 Weak Form and Finite Element Approximation

In order to obtain the numerical solution using the finite element method, the weak form of equilibrium equations is formulated as:

$$G = \int_A \left(\boldsymbol{N}.\delta\boldsymbol{e} + \sum_{k=1}^{2} \left(\boldsymbol{M}_k.\delta\boldsymbol{\chi}^k\right) + \boldsymbol{T}_1.\delta\gamma^1 + \widetilde{\boldsymbol{q}}.\delta\boldsymbol{E} \right) dA - G_{ext} = 0 \tag{6}$$

where $\boldsymbol{N}$, $\boldsymbol{M}_k$ and $\boldsymbol{T}_1$ represent the membrane, bending and shear stresses resultants respectively. $\widetilde{\boldsymbol{q}}$ is the electric displacement and $\boldsymbol{G}_{ext}$ is the external virtual work. These vectors can be written in the form:

$$\boldsymbol{N} = \int_{-h/2}^{h/2} \begin{bmatrix} \sigma_{11} \\ \sigma_{22} \\ \sigma_{12} \end{bmatrix} dz,\ \boldsymbol{M}_k = \int_{-h/2}^{h/2} f_k(z) \begin{bmatrix} \sigma_{11} \\ \sigma_{22} \\ \sigma_{12} \end{bmatrix} dz$$

$$\boldsymbol{T}_1 = \int_{-h/2}^{h/2} f_1'(z) \begin{bmatrix} \sigma_{13} \\ \sigma_{23} \end{bmatrix} dz,\ \widetilde{\boldsymbol{q}} = \int_{-h/2}^{h/2} \boldsymbol{q}\, dz\ ,\ k = 1, 2 \tag{7}$$

The generalized resultant of stress and strain vectors are expressed as

$$\boldsymbol{R} = [\boldsymbol{N} \quad \boldsymbol{M}_1 \quad \boldsymbol{M}_2 \quad \boldsymbol{T}_1 \quad \widetilde{\boldsymbol{q}}]^T_{14\times1},\ \boldsymbol{\Sigma} = \left[\boldsymbol{e} \quad \boldsymbol{\chi}^1 \quad \boldsymbol{\chi}^2 \quad \boldsymbol{\gamma}^1 \quad -\boldsymbol{E}\right]^T_{14\times1} \tag{8}$$

The linear constitutive equations of piezoelasticity expressing the coupling between the elastic and electric fields relevant to present problem can be defined as:

$$\begin{cases} \boldsymbol{\sigma} = \boldsymbol{C}\, \boldsymbol{\varepsilon} - \boldsymbol{p}^T\, \boldsymbol{E} \\ \boldsymbol{q} = \boldsymbol{p}\, \boldsymbol{\varepsilon} + \boldsymbol{k}\, \boldsymbol{E} \end{cases} \tag{9}$$

Using Eqs. (6) and (9), the stress resultant $\boldsymbol{R}$ is related to the strain field.

$$\boldsymbol{R} = \boldsymbol{H}_T\boldsymbol{\Sigma},\ \boldsymbol{H}_T = \begin{bmatrix} \boldsymbol{H}_{11} & \boldsymbol{H}_{12} & \boldsymbol{H}_{13} & 0 & \boldsymbol{H}_{15} \\ & \boldsymbol{H}_{22} & \boldsymbol{H}_{23} & 0 & \boldsymbol{H}_{25} \\ & & \boldsymbol{H}_{33} & 0 & \boldsymbol{H}_{35} \\ & & & \boldsymbol{H}_{44} & \boldsymbol{H}_{45} \\ Sym & & & & \boldsymbol{H}_{55} \end{bmatrix} \tag{10}$$

with $\boldsymbol{H}_T$ is the linear coupling elastic and electric matrix expressed as:

$$\begin{cases} (\boldsymbol{H}_{11}, \boldsymbol{H}_{12}, \boldsymbol{H}_{13}, \boldsymbol{H}_{22}, \boldsymbol{H}_{23}, \boldsymbol{H}_{33}) = \int_{-h/2}^{h/2} \left(1, f_1, f_2, f_1^2, f_1 f_2, f_2^2\right) \boldsymbol{C} dz \\ \boldsymbol{H}_{44} = \int_{-h/2}^{h/2} \left(f_1'\right)^2 \boldsymbol{C}_\tau\, dz \\ (\boldsymbol{H}_{15}, \boldsymbol{H}_{25}, \boldsymbol{H}_{35}) = \int_{-h/2}^{h/2} (1, f_1, f_2) \boldsymbol{p}_1^T\, dz \\ \boldsymbol{H}_{45} = \int_{-h/2}^{h/2} f_1' \boldsymbol{p}_2^T dz \\ \boldsymbol{H}_{55} = \int_{-h/2}^{h/2} \boldsymbol{k}\, dz \end{cases} \tag{11}$$

where $\boldsymbol{C}$ and $\boldsymbol{C}_\tau$ are in plane and out-of-plane linear elastic sub-matrices. $\boldsymbol{p}_1^T$, $\boldsymbol{p}_2^T$ and $\boldsymbol{k}$ represent the in plane and out-of-plane piezoelectric coupling sub-matrices and dielectric permittivity matrix, respectively.

In the finite element approximation, the geometry, the displacements and the electric potential are approximated by means of the isoparametric concept. The double director vectors $\delta \boldsymbol{d}_1$ and $\delta \boldsymbol{d}_2$ are approximated with the same functions as in (Mallek et al. 2018). Therefore, the discrete form of Eq. (7) leads to the discretized static linear piezoelastic equilibrium equation for the structure.

3 Numerical Results

In this section, the static behavior of adaptive composite with surface bonded actuators/sensor is performed to demonstrate the accuracy and the performance of the proposed piezoelectric shell element. A simply supported cross-ply square made of S-glass/Epoxy, with the internal sequence of layers [45°/−45°/45°], acts as actuators and sensors. Two piezoelectric layers, made of PXE-52, bonded to the top and bottom surfaces. The side dimension is a = 0.1 m, the thickness of each S-glass/Epoxy layer is 0.0004 m and of active layer is 0.0002 m. The material properties of S-glass/Epoxy used for the calculation are $Y_1 = 55\,\text{GPa}$, $Y_2 = 16\,\text{GPa}$, $G_{12} = 7.6\,\text{GPa}$, $v_{12} = 0.28$. The material and piezoelectric properties of PXE-52 are: $Y_1 = Y_2 = 62.5\,\text{GPa}$, $G_{12} = 24\,\text{GPa}$, $v_{12} = 0.3$, $e_{11} = e_{22} = -280.10^{-12}\,\text{m/V}$ and $p_{33} = -3.45^{-8}\,\text{F/m}$. An 8×8 finite element mesh is applied.

Case 1: Sensing:

The plate is studied as a sensor case (see Fig. 1). Deformation caused by external mechanical loads results in electric charges due to the direct piezoelectric effect. A uniformly distributed load $L_{mech} = \mu p_o$ (μ represents the load level) is initially subjected to the plate, which leads to a linear distribution of the bending moment along the length, where $p_0 = 10\,\text{kN/m}^2$. The present predictions and solutions provided by Moita et al. (2002) are shown in Table 1. The results are in good agreement with the alternative solutions.

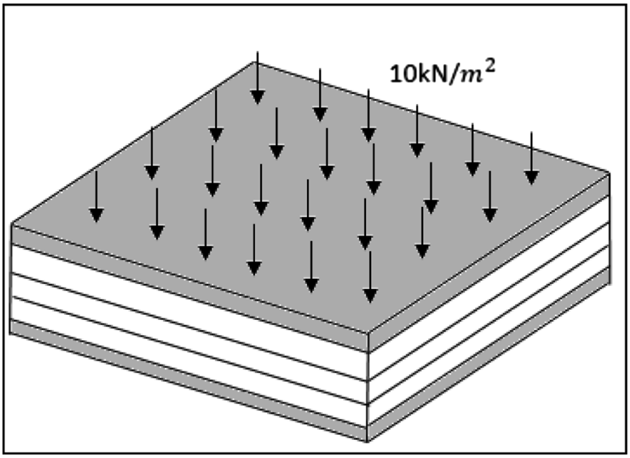

Fig. 1. Adaptive composite plate under mechanical load.

Table 1. Central deflection W_c [mm] for different mechanical loads.

Load level μ	Mechanical load $L_{mech} = \mu\, p_0$	
	(a)	(b)
0.5	0.1085	0.1096
1.0	0.2170	0.2193
1.5	0.3255	0.3290
2.0	0.4340	0.4386
2.5	0.5425	0.5483
3.0	0.6510	0.6580

(a) Moita et al. (2002); (b) Present Model

Case 2: Actuation:

Starting from $\varphi_0 = \pm 135.35\,\mathrm{V}$, an increase in the potential voltage up to $\varphi = \pm 454.05\,\mathrm{V}$ is applied across the thickness, the induced internal stresses result in a bending moment which causes deflection of the plate. The center deflection W_c of simply supported composite plate is depicted in Fig. 2 for different load levels, defined by $\mu = L_{electr}\varphi_0$. The obtained results are in good agreement with the alternative linear solution obtained by Moita et al. (2002), using Kirchhoff classical piezo-laminated 3-node plate/shell element.

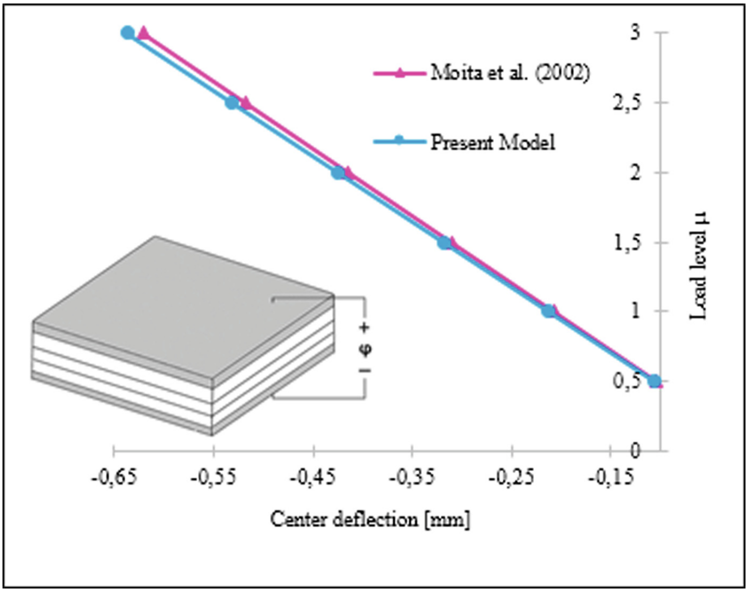

Fig. 2. Center deflection of the adaptive composite plate under different electric loads.

4 Conclusion

This paper presents a developed finite element model based on a discrete double-directors shell elements that can be gainfully used for modeling and simulation of the behavior of smart structure with integrated sensors/actuators. The electric potential is assumed to be a linear function through the thickness of each active sub-layer. The static behavior is performed in terms of deflection with varying the load level. The validation of the present model is based on comparing the obtained results to the literature once for a simply supported laminated plate subjected to mechanical and electric load. A good agreement is obtained between the present results and the reference results.

References

Chesne, S., Pezerat, C.: Distributed piezoelectric sensors for boundary force measurements in Euler-Bernoulli beams. Smart Mater. Struct. **20**(7), 075009 (2011)

Correia, I.F.P., Soares, C.M.M., Soares, C.A.M., Herskovits, J.: Active control of axisymmetric shells with piezoelectric layers: a mixed laminated theory with a high order displacement field. Comput. Struct. **80**, 2256–2275 (2002)

Foda, M.A., Almajed, A.A., ElMadany, M.M.: Vibration suppression of composite laminated beams using distributed piezoelectric patches. Smart Mater. Struct. **19**(11), 115018 (2010)

Frikha, A., Wali, M., Hajlaoui, A., Dammak, F.: Dynamic response of functionally graded material shells with a discrete double directors shell element. Compos. Struct. **154**, 385–395 (2016)

Gabbert, U., Koppe, H., Seeger, F., Berger, H.: Modeling of smart composite shell structures. J. Theoret. Appl. Mech. **40**(3), 575–593 (2002)

Jrad, H., Mallek, H., Wali, M., Dammak, F.: Finite element formulation for active functionally graded thin-walled structures. Comptes Rendus Mec. **346**(12), 1159–1178 (2018)

Lammering, R., Yang, F.: A four-node finite element for piezoelectric shell structures in convective coordinates. Mech. Adv. Mater. Struct. **16**, 198–209 (2009)

Mallek, H., Jrad, H., Algahtani, A., Wali, M., Dammak, F.: Geometrically non-linear analysis of FG-CNTRC shell structures with surface-bonded piezoelectric layers. Comput. Methods Appl. Mech. Eng. **347**, 679–699 (2019a)

Mallek, H., Jrad, H., Wali, M., Dammak, F.: Geometrically nonlinear finite element simulation of smart laminated shells using a modified first-order shear deformation theory. J. Intell. Mater. Syst. Struct. (2018). https://doi.org/10.1177/1045389x18818386

Mallek, H., Jrad, H., Wali, M., Dammak, F.: Piezoelastic response of smart functionally graded structure with integrated piezoelectric layers using discrete double directors shell element. Compos. Struct. **210**, 354–366 (2019b)

Marinković, D., Koppe, H., Gabbert, U.: Numerically efficient finite element formulation for modeling active composite laminates. Mech. Adv. Mater. Struct. **13**, 379–392 (2006)

Marinković, D., Rama, G.: Co-rotational shell element for numerical analysis of laminated piezoelectric composite structures. Compos. Part B Eng. **125**, 144–156 (2017)

Mellouli, H., Jrad, H., Wali, M., Dammak, F.: Meshless implementation of arbitrary 3D-shell structures based on a modified first order shear deformation theory. Comput. Math Appl. **77**, 34–49 (2019a)

Mellouli, H., Jrad, H., Wali, M., Dammak, F.: Meshfree implementation of the double director shell model for FGM shell structures analysis. Eng. Anal. Bound. Elem. **99**, 111–121 (2019b)

Moita, J.M.S., Soares, C.M.M., Soares, C.A.M.: Geometrically non-linear analysis of composite structures with integrated piezoelectric sensors and actuators. Compos. Struct. **57**(1–4), 253–261 (2002)

Neto, M.A., Leal, R.P., Yu, W.: A triangular finite element with drilling degrees of freedom for static and dynamic analysis of smart laminated structures. Compos. Struct. **108–109**, 61–74 (2012)

Rama, G.: A 3-node piezoelectric shell element for linear and geometrically nonlinear dynamic analysis of smart structures. Facta Univ. Ser. Mech. Eng. **15**(1), 31–44 (2017)

Rama, G., Marinković, D., Zehn, M.: Efficient three-node finite shell element for linear and geometrically nonlinear analyses of piezoelectric laminated structures. J. Intell. Mater. Syst. Struct. **29**(3), 345–357 (2018)

Sudhakar, A.K., Kamal, M.: Finite element modeling of smart plates/shells using higher order shear deformation theory. Compos. Struct. **62**, 41–50 (2003)

Trabelsi, S., Frikha, A., Zghal, S., Dammak, F.: Thermal post-buckling analysis of functionally graded material structures using a modified FSDT. Int. J. Mech. Sci. (2018). https://doi.org/10.1016/j.ijmecsci.2018.05.033

Valvano, S., Carrera, E.: Multilayered plate elements with node-dependent kinematics for the analysis of composite and sandwich structures. Facta Univ. Ser. Mech. Eng. **15**(1), 1–30 (2017)

Wali, M., Hentati, T., Jaraya, A., Dammak, F.: Free vibration analysis of FGM shell structures with a discrete double directors shell element. Compos. Struct. **125**, 295–303 (2015)

Wu, X.H., Chen, C., Shen, Y.P., Tian, X.G.: A high order theory for functionally graded piezoelectric shells. Int. J. Solids Struct. **39**, 5325–5344 (2002)

Zghal, S., Frikha, A., Dammak, F.: Static analysis of functionally graded carbon nanotube-reinforced plate and shell structures. Compos. Struct. **176**, 1107–1123 (2017)

Zhang, W.M., Tabata, O., Tsuchiya, T., Meng, G.: Noise-induced chaos in the electrostatically actuated MEMS resonators. Phys. Lett. A **375**(32), 2903–2910 (2011)